Highlights

Ecosystem services and management of reed and seagrass debris on a urban Mediterranean beach (Poetto, Italy)

Andrea Ruju, Carla Buosi, Giovanni Coco, Marco Porta, Daniele Trogu, Angelo Ibba, Sandro De Muro

- A numerical approach assesses runup on a beach with seagrass wracks
- Large permeability values were measured in areas with seagrass and reed deposits
- Infiltration processes allow the beach to drain the overwashed water
- Reed and seagrass wracks can mitigate flooding by increasing beach permeability

Ecosystem services and management of reed and seagrass debris on a urban Mediterranean beach (Poetto, Italy)

Andrea Ruju[a], Carla Buosi[b], Giovanni Coco[c], Marco Porta[b], Daniele Trogu[b], Angelo Ibba[b], Sandro De Muro[b]

[a] *Dipartimento di Ingegneria Civile, Ambientale e Architettura, University of Cagliari, Cagliari, 09123, Italy*
[b] *Coastal and Marine Geomorphology Group (CMGG), Dipartimento di Scienze Chimiche e Geologiche, University of Cagliari, Monserrato, 09042, Italy*
[c] *School of Environment, University of Auckland, Auckland, 1010, New Zealand*

Abstract

This paper reports a scientific inquiry carried out within the management process of an exceptional accumulation of reeds and seagrasses that took place in December 2019 on Poetto beach (Cagliari, southern Sardinia, western Mediterranean). The magnitude of the event raised concern within the local community and tourism service providers especially for the compromised beach accessibility caused by this large amount of biomass. The scientific inquiry is carried out in support of coastal management, to assess the berm processes before the removal of the reed wracks decided by the local municipality. By means of a numerical approach, this work devotes special attention to the runup induced by storms in the presence of reed and seagrass deposits on a low-lying backshore. Field surveys reported relatively large conductivity parameters in the presence on reed and seagrass deposits. The numerical approach shows that the increased beach permeability can eventually mitigate coastal flooding induced by storms. These results highlight the ecosystem services provided by reed and seagrass wracks together with the implications for coastal protection and management.

Keywords: Coastal Flooding, Seagrass deposits, Ecosystem Services, Wave Modelling, Beach Resilience
PACS: 0000, 1111
2000 MSC: 0000, 1111

---

1. Introduction

Worldwide shorelines are often littered with biomass originating from terrestrial and marine ecosystems [1]. Regardless of its origin, this material is ultimately deposited on the backshore by waves under storm conditions. Recent work has addressed the role of woody debris in coastal processes such as dune evolution and growth [2, 3]. These studies have shown that dead trees and large logs (commonly referred to as driftwood) are a significant agent affecting morphodynamics of sandy beaches subject to appreciable aeolian sand transport. In fact, foredune development can benefit from the presence of woody debris that promote accumulation of windblown sand in the backshore. Moreover, Kennedy and Woods [4] suggest that woody debris act as a buffer to waves during storm events on gravel beaches.

Posidonia oceanica meadow is another source of biomass, along Mediterranean and southwestern Australian coastlines [5, 6], that storms uproot and transport from the shoreface, eventually accumulating it on the backshore [7]. The presence of seagrass necromass (leaves and rhizomes mixed with sand, commonly referred to as banquette or beach-cast litter) mitigates beach erosion induced by winter storms by promoting sediment retention and reducing sediment resuspension [8, 9].

The aforementioned work has contributed to the characterization of coastal processes induced by large woody debris and *Posidonia oceanica* banquettes, drawing attention to their ecosystem services. However, beside the services identified by the scientific community, the presence of this biomass often poses a management issue especially on beaches devoted to tourism. For instance, despite being a common feature on Mediterranean beaches, the *Posidonia oceanica* banquette is not always perceived positively by tourism service providers and beach-goers [10]. This has led local authorities to prepare guidelines devoted to the identification of strategies for the management of banquettes. Due to its recognized services offered in terms of coastal protection, in Italy the regulation of *Posidonia oceanica* falls within the exclusive competence of the state legislator. The regional legislative competence in the field of tourism can be exercised, only insofar as it is not in contrast with the state discipline. In Sardinia, the 2016 regional resolution (40/13 of 6.7.2016) entitled "Operational guidelines for the management of *Posidonia oceanica* deposits on beaches" suggests that the preferred management strategy is to keep the wracks on site. In the event that, for technical reasons that objectively hinder the usability of the beach in the summer season, keeping the

Posidonia deposits on site is extremely problematic, the option of moving and subsequent repositioning of the accumulations and the transfer to waste disposal or recovery plants can be pursued following some procedural and operating instructions.

Large woody debris and *Posidonia oceanica* wracks are not the only source of biomass on Mediterranean beaches. Small and medium-size woody debris, such as reeds proceeding from fluvial systems, are a common feature whose role in beach morphodynamics has received less attention by the scientific community [11]. In particular, to the best of the authors' knowledge, a quantitative assessment of the role played by beach berms reinforced by seagrass and reed wracks on the protection of sandy beaches has not been reported. Moreover, probably due to the rarity of large reed deposition events, the management of these deposits is less regulated than the case of *Posidonia oceanica*. The absence of regulation leaves coastal managers without clear guidelines for the management of reed deposits on beaches.

This paper reports the scientific inquiry carried out within the management process of an exceptional accumulation of reeds (*Arundo donax* proceeding from local fluvial systems) and seagrasses on the berm of Poetto beach (Cagliari, Southern Sardinia). Although reed deposition on Poetto beach is not unusual, an exceptional event occurred on December 2019 with a magnitude that had not been previously observed. The great amount of this biomass accumulated nearby the shoreline raised concerns especially among local tourism service providers, worried about its negative impacts. The municipality of Cagliari disposed the measures to bring the beach back to the previous state and, due to the absence of a legislation on the management of reed deposits, commissioned the CMGG (Coastal and Marine Geomorphology Group) of the University of Cagliari to prepare a scientific inquiry, including the monitoring of the beach berm processes before, during and after the removal of reeds. The main purpose of the inquiry is thus to scientifically support and motivate the management decisions.

A special attention in the scientific inquiry is devoted to runup and flooding on Poetto beach, characterized by low-lying sandy backshore and the implications for coastal protection and management. The shape of Poetto beach profile, with a berm higher than a large portion of the emerged beach, allows to consider the implications of using vertical and horizontal runup values in the assessment of beach flooding. The runup assessment conducted through a numerical approach benefited from the preparatory field work, including beach surveys and permeability tests. Beach surveys reported large spatial variability of hydraulic conductivity across the beach, related to the distribution of reed and seagrass deposits within the sediment. The role of infiltration/exfiltration processes on a low-lying sandy beach under overwash events is investigated in detail. For this purpose, we identified the major storms that hit the study area during the monitoring period to assess the storm-induced coastal flooding through numerical modelling including groundwater flow processes.

The paper is structured as follows. Sections 2 and 3 introduce the geographical settings together with the event which drove the reed deposition on the beach berm. Section 4 describes the monitoring program along with the numerical approach. Section 5 reports the results from the hydrodynamic modelling. Section 6 discusses the results and Section 7 draws some conclusions.

2. Geographical settings

Poetto beach lies in the innermost part of the Gulf of Cagliari, Southern Sardinia (Italy), inside the metropolitan area of Cagliari (Figure 1). It is a micro-tidal urban sandy beach with a length of 8 km and a maximum width of about 100 m. The beach is backed by a relatively narrow primary dune system (foredunes and embryo dunes) bordered by a residential neighborhood and a 4-lane motorway that connects the two main towns of the metropolitan area: Cagliari and Quartu Sant'Elena. Moreover, from the administrative point of view, the beach is divided into two sectors of similar size: the municipality of Cagliari manages the western sector whereas Quartu Sant'Elena manages the eastern part. A nourishment project carried out in 2002 in the Cagliari municipality sector has significantly modified the textural, compositional and morphological features of the backshore, shoreline and shoreface [12]. Besides, an increasing anthropic pressure, mainly related to the touristic sector, is responsible for an impact on the beach system, significantly affecting morphodynamic processes [13].

Wave conditions along Poetto beach system result from a combination of Mediterranean swells and locally-generated wind waves, with directions mainly ranging from South-East to South-South-West, see the wave rose in Figure 1. The Copernicus Marine Environment Monitoring Service (CMEMS) database covering the period 2006-2018 gives a mean significant wave height H_s of 0.4 m at the virtual buoy in front of the beach. Scirocco storm events drive the most intense swells that hit the beach from South-East and South-

South-East directions. Moreover, the South-South-West sector contains considerable wave energy that is mainly related to West-South-West swells that enter the Gulf of Cagliari. Under these conditions, the wave direction in front of Poetto beach is the result of the shelter offered by Capo Spartivento (the Southernmost promontory of Sardinia) and wave refraction in the nearhsore. The emerged beach of Poetto is periodically flooded by South-East storms, with a flooding extension that episodically can reach the coastal street and nearby proprieties [12].

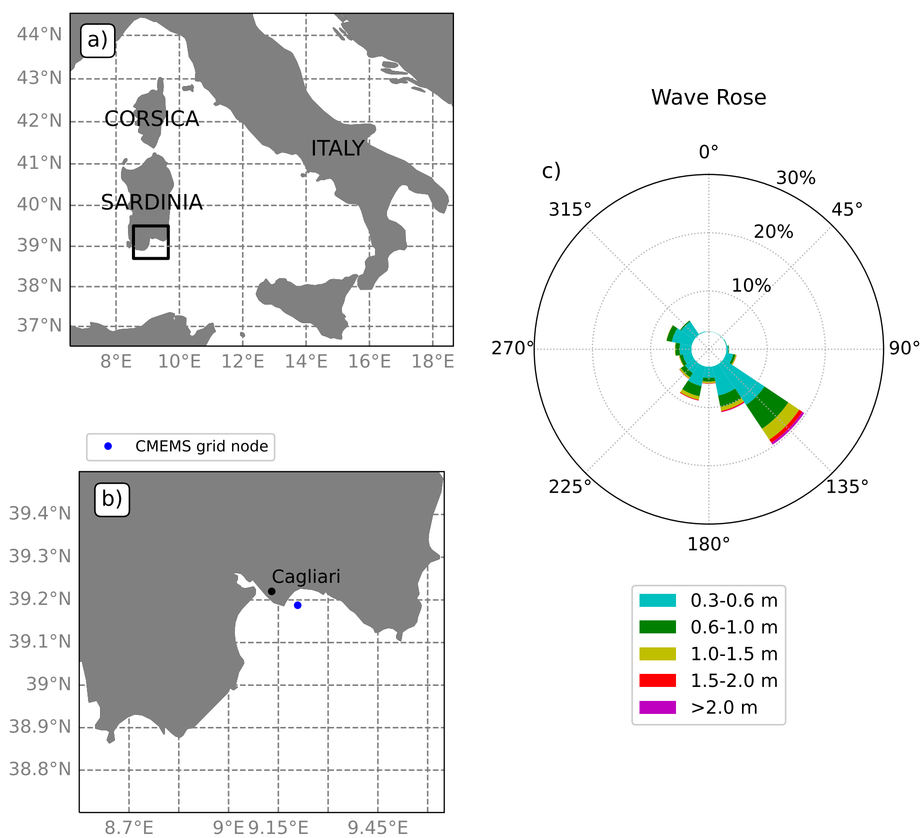

Figure 1: a) and b) Geographical settings with the location of the virtual buoy in front of the Poetto beach indicated by the blue dot in panel b). c) Wave rose at the virtual buoy from the CMEMS database (2006-2018).

3. Event analysis

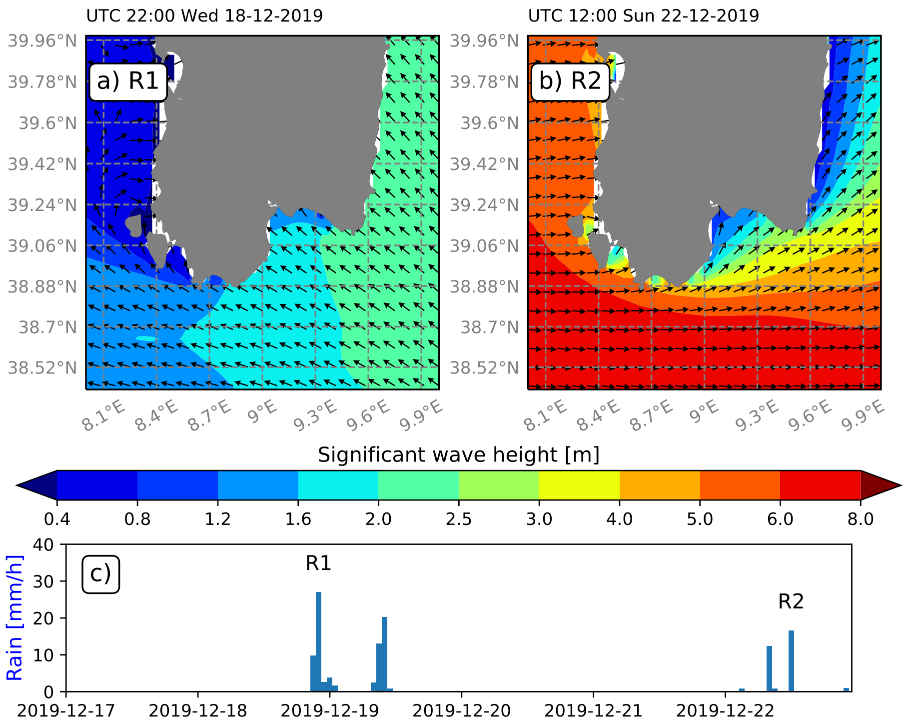

Figure 2: a) and b) Significant wave height during the two events R1 and R2 that drove the reed deposition and redistribution along the Poetto beach (Wave data from the CMEMS database). c) Precipitation rate measured at the Poetto beach.

Heavy rain precipitation events occurred between the 18/12/2019 and the 22/12/2019 in the metropolitan area of Cagliari. The meteorological station located on the roof of a building in close proximity to the Poetto beach recorded precipitation peaks above 25 mm/h between 18:00h and 24:00h of the 18/12/2019 (the average yearly total precipitation is on the order of 500 mm in Cagliari). This weather events triggered a rapid increase of runoff discharged by surface streams to the Gulf of Cagliari. The resulting flows were able to put in motion and transport to the sea a considerable amount of biomass. The upper panels of Figure 2 displays the wave propagation in the Gulf of Cagliari at the moment of the two rain peaks indicated as R1 and R2 in the lower plot.

Once it reached the sea, this biomass, made mostly up of uprooted reeds (*Arundo donax*) from local streams, was transported and spread by marine currents and waves driven by the energetic South-East swell that battered Southern Sardinia coasts during these days. Figure 2a shows that the significant wave height was above 1.5 m in the nearshore of the Gulf of Cagliari. Few days later the event that triggered the reed transport to the sea, a massive South-West storm approached the southern Sardinian coasts. Significant wave heights of above 6 m were expected on the western coasts of the islands of San Pietro and Sant'Antioco. This massive swell, although attenuated by the shelter offered by Capo Spartivento (the southernmost Sardinian land), entered the Gulf of Cagliari and played a role in the redistribution of reeds along the shore, see Figure 3a. Figure 2c shows the evolution of the rain rate during the third week of December 2019, together with the significant wave height maps during the two rain rate peaks identified as R1 and R2 in the figure. The precipitation was measured by a meteorological station managed by the CMGG, located on the roof of a hospital immediately behind Poetto beach. Wave data proceed from the CMEMS database that uses the spectral wave model WAM to simulate the wave evolution with a spatial resolution of $1/25^o$ of latitude and a time resolution of 1 hour.

The great amount of biomass accumulated on the shoreline raised concerns especially among local tourism service providers, worried about its negative impacts in terms of beach accessibility. Due to the absence of legislation and the strategic importance of the beach for the local community, the municipality of Cagliari involved stakeholders, the University and local authorities in the decision making process with the objective of identifying a shared strategy about the management of this exceptional event. Once the options of 1) keeping the deposits on site and 2) their temporal movement have been considered as not viable options, the municipality of Cagliari disposed the measures to remove the reed deposits from the beach and commissioned the CMGG group of the University of Cagliari for the monitoring of the beach berm processes. Following the suggestion made by the CMGG and in agreement with the guidelines listed by the Sardinian legislation for the *Posidonia oceanica* management, the municipality disposed that the removal operations of reed berms should have been carried out in a sustainable way, preserving the natural characteristics of the beach. In fact, the reeds were removed manually (see Figure 3b) avoiding the use of heavy machinery that usually causes a considerable loss of sediments, resulting in changes in the beach morphology (e.g., flattening of the beach profile, sediment compacting and obliteration of sedimentary features like berms, beach-face steps, etc).

The management of this local exceptional event was affected by a larger global exceptional event: the corona virus (COVID-19) emergency. To contain the emergency, in March 2020 the Italian government imposed a national lockdown with strong restrictions on economic activities and the closure of beaches to public access. The lockdown lasted until May 2020 and under this period scientists had the unprecedented opportunity to observe ecosystem dynamics with almost no human interference. The beach berm reinforced by the presence of reeds stayed in place until its removal that occurred in April and May 2020.

4. Methods

4.1. Monitoring program

The monitoring of the eco-geomorphological dynamics at Poetto beach included actions before and after the reeds removal: topographic and bathymetric surveys, collection of the rectified images through the videomonitoring system and permeability tests. This section describes only the topographic/bathymetric surveys and the permeability tests.

The topographical surveys were carried out along two transects in the western sector of the beach. Data were collected using DGPS in a GNSS (Global Navigation Satellite System) at frequency of 1 Hz. The transects run over the emerged beach from the dune system to the shallow shoreface at about one meter depth. The shoreface bathymetry along each transect was recorded using a single-beam echo-sounder coupled with a DGPS receiver interacting with a navigation software (frequency of 5 Hz). The topographic and bathymetric data were combined to obtain a morphological profile of the emerged and submerged beach, from the dune system up to the upper limit of the *Posidonia oceanica* meadow (depths 10-15 m at Poetto). Figure 4 shows the beach profiles surveyed along the two transects T3 and T7 before the removal of the reeds. In Figure 4c it is also possible to identify the upper limit of the *Posidonia oceanica* meadow that lies where the profile becomes noisy due to the presence of seagrass below 8/10 m depth for transects T7.

Infiltrometric tests conducted with double-ring infiltrometers allowed the characterization of the hydraulic conductivity on the sandy beach and on the beach berm with banquette. The permeability coefficients on sand ranged between 0.00003 m/s on the backshore and 0.0003 m/s on the beach berm

Figure 3: a) Reed accumulation on the berm of Poetto beach. b) Removal operations of reed deposits.

with buried reeds. Larger permeability coefficients were measured on the beach berm with seagrass litter: they ranged between 0.14 and 0.15 m/s.

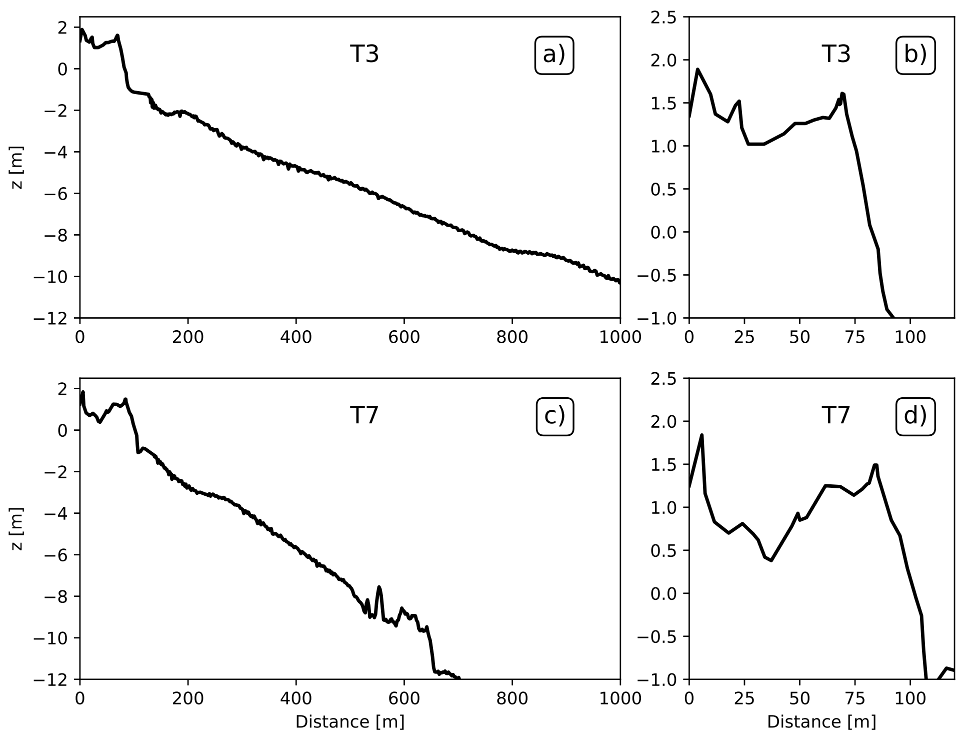

Figure 4: a) and c) Beach profiles along the two transects T3 and T7. b) and d) Details of the foreshore and emerged beach profiles.

4.2. Storm identification

Incoming wave conditions at Poetto beach, for the period comprised between the deposition of reeds in December 2019 and their complete removal in May 2020, were collected from the CMEMS hindcast time series [14]. For this purpose we chose the grid node of the computational domain located in front of Poetto beach. Figure 1b shows the location of the CMEMS system grid node indicated as virtual buoy, whereas Figure 5 plots the time series of the incident wave parameters at that location: significant wave height

(H_s), mean period (T_m) and mean direction (θ). Panel d) of Figure 5 shows the mean sea level (msl) evolution recorded by the tide gauge located inside the Cagliari harbour, 4 km away from the Poetto beach. The analysis of the evolution of the significant wave height highlights several storms, among which it is possible the identification of the two storms that drove the reed deposition and their following redistribution along the Poetto beach in the month of December 2019. The most intense storm in the observation period occurred from the 20th to the 23th of January 2020 (with a peak on the evening of the 21st of January with significant wave heights of 2.9 m).

We used the peak-over-threshold (POT) [15] method to identify the 48-h independent storms occurred during the observation period at the virtual buoy location represented by the CMEMS grid node. We identified the storms based on the prominence parameter for the significant wave height H_s: the prominence threshold was chosen equal to 0.6 m. Although the threshold value of 0.6 m may seem low for extreme event analysis, due to the moderate incoming wave energy levels at Poetto (mean H_s is 0.4 m), this method allowed the identification of 12 storms during the five-month period considered. We retained only the storms with a persistence above the threshold longer than 6 h, that met the independence criterion with more than 48 h between the peak of a storm and the peak of the following one. The extreme wave parameters representative of each storm of the sample were selected as the values occurring at the time in which the maximum wave height was observed during the storm duration. Table 1 reports the dates of occurrence together with the wave parameters and the mean sea level of the identified 12 storms. The last column of the table lists the effects observed from the video monitoring system.

4.3. Modelling approaches

4.3.1. Phase-averaged modelling

To evaluate the role played by the organic berm in coastal protection from flooding, the incident wave conditions collected at the nearshore grid nodes of the CMEMS system were numerically propagated in the nearshore with the SWAN model [16]. The SWAN model is a spectral wave model based on the wave action equation. It is nowadays widely used to address wave nearshore processes [17, 18]. The wave spectra reconstructed at six nodes of the CMEMS system represented the wave conditions imposed at the boundary of the numerical grid used for the wave propagation with SWAN (Figure 6). The six grid nodes lie along the open SWAN boundaries at West, South

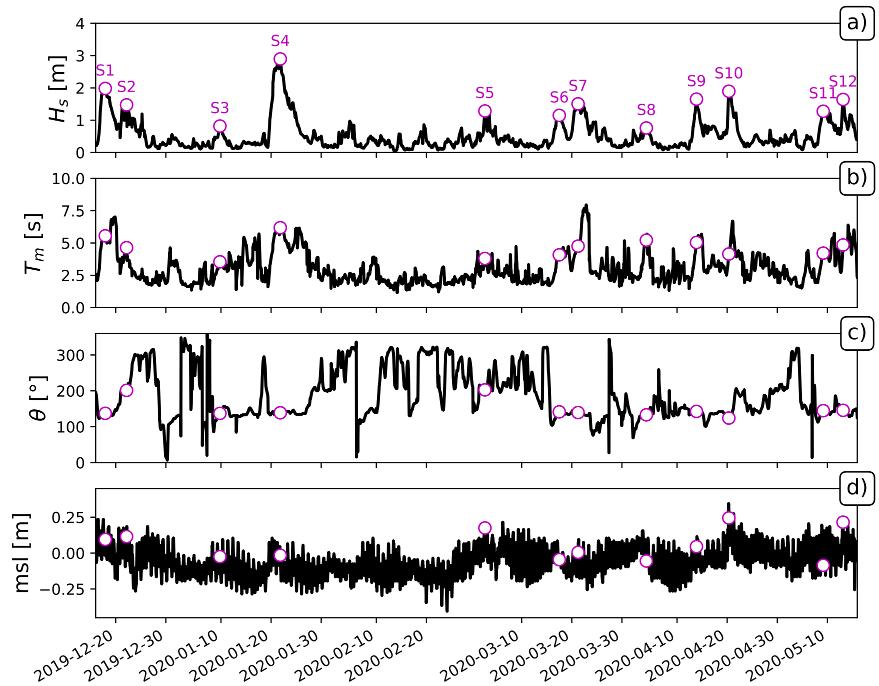

Figure 5: Time series of wave parameters and mean sea level at the Poetto beach during the observation period. a) Significant wave height, b) mean period, c) mean wave direction, d) mean sea level. The circles highlights the main storm events.

and Est of the grid. The spectral reconstruction routine was necessary since CMEMS does not provide the full frequency-directional spectra but it makes available the partition parameters (H_s,T_m and θ) for two swells and one wind sea component. The partition parameters from CMEMS were used to reconstruct the full spectra at the boundary nodes. For this purpose we inferred the full frequency-directional spectrum as a sum of the three partitioned spectra (primary and secondary swell and wind wave component) reconstructed from the partition parameters, assigning a parametric spectral shape (JONSWAP) with a large directional spread to the wind wave component with respect to the swell components. The routine of spectrum reconstruction at

Storm	Date	Hour	H_s [m]	T_p [s]	T_m [s]	Dir [o]	msl [m]	Effects
S1	2019-12-17	22:00	1.98	8.39	5.56	137.30	0.09	overwash
S2	2019-12-22	04:00	1.48	11.17	4.64	201.35	0.11	none
S3	2020-01-09	19:00	0.82	5.73	3.54	137.14	-0.02	none
S4	2020-01-21	20:00	2.90	8.39	6.18	138.90	-0.02	overwash
S5	2020-03-02	16:00	1.29	5.73	3.80	202.74	0.17	none
S6	2020-03-17	12:00	1.15	6.93	4.08	141.53	-0.05	none
S7	2020-03-21	06:00	1.51	7.63	4.76	139.53	0.01	none
S8	2020-04-03	21:00	0.76	8.39	5.22	133.24	-0.05	none
S9	2020-04-13	21:00	1.65	6.93	5.04	142.70	0.04	none
S10	2020-04-20	08:00	1.90	7.63	4.15	124.24	0.24	overwash
S11	2020-05-09	04:00	1.28	6.30	4.22	144.79	-0.09	none
S12	2020-05-13	03:00	1.64	6.93	4.85	145.67	0.21	none

Table 1: Wave parameters and mean sea level during the storms occurred in the period December 2019-May 2020 at Poetto beach. The last column lists the effects observed from the video monitoring system.

each node can be summarized as follows:

- reconstruction of the frequency-directional spectrum with JONSWAP shape (γ=3.3) and directional spread of 19^o from the bulk wave parameters of the primary swell partition provided by CMEMS
- reconstruction of the frequency-directional spectrum with JONSWAP shape (γ=3.3) and directional spread of 19^o from the bulk wave parameters of the secondary swell partition provided by CMEMS
- reconstruction of the frequency-directional spectrum with JONSWAP shape (γ=3.3) and directional spread of 25^o from the bulk wave parameters of the wind-wave partition provided by CMEMS
- the total spectrum is the sum of the three previous spectra

This routine with the spectrum reconstruction from wave spectral partitions represents an improvement with respect to the reconstruction from total bulk wave parameters (adopted, for instance, by [17]) since it allows the characterization of multi-modal seas. Figure 7 shows the result of the spectral reconstruction routine for storm S12. From the comparison of panels a) and c) it is possible to appreciate the different shapes of the swell and the wind

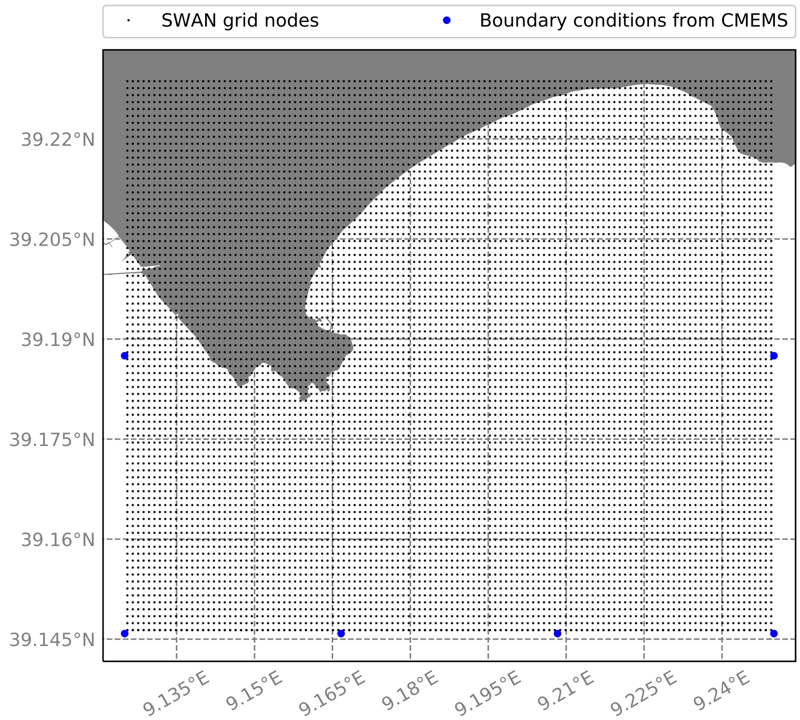

Figure 6: Computational grid domain in SWAN. The blue points are the CMEMS grid nodes in which the boundary conditions for SWAN are reconstructed.

wave spectra with the latter characterized by a larger directional spread. Panel b) suggests that for storm S12 the secondary swell virtually carry no energy, which is a common situation in a closed basin as it is the Mediterranean Sea. As a result, the total spectrum for storm S12 is simply given by the sum of the primary swell (the secondary swell is close to zero) and the wind wave spectra.

The grid used in the SWAN simulation (Figure 6) has a spatial resolution of 1/16 of nautical mile (about 115 m) and allows the achievement of the wave conditions in the proximity of Poetto beach and the identification of the main wave transformation processes in coastal water.

The reliability of the spectral wave modelling approach is assessed by comparing the SWAN output with wave measurements in coastal water. Since we do not have measurements available in the observation period, we use the data collected by an AWAC (Acoustic Wave And Current) profiler deployed

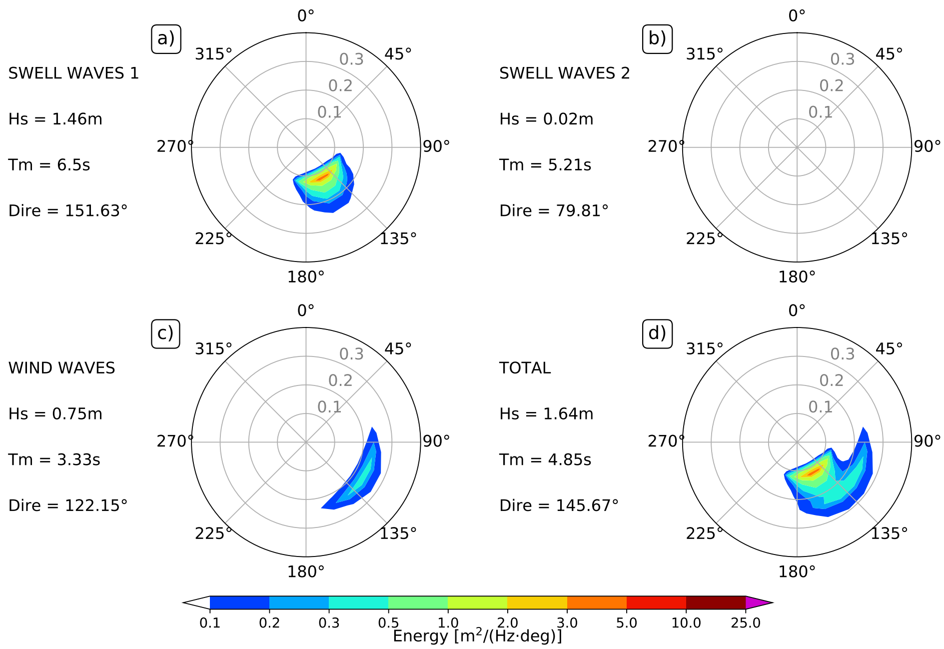

Figure 7: Reconstruction of spectral wave boundary conditions (storm S12) from bulk swell and wind wave parameters. a) Primary swell wave spectrum, b) secondary swell wave spectrum, c) wind wave spectrum, d) total wave spectrum.

in the nearshore of Poetto at a water depth of 18 m during two field campaigns conducted, respectively, in Spring 2017 and Fall 2020. Further details about the field campaign and the exact AWAC location can be found in Ruju et al. [19]. The adoption of the procedure described in section 4.2 allows the identification of 5 wave events, whose H_s is between 0.9 and 2.8 m. These events are simulated with SWAN following the routine described in section 4.3.1. Here, we adopt the normalized root- mean-square-error $NRMSE$, defined as follows:

$$NRMSE = \sqrt{\frac{\sum(O_i - M_i)^2}{\sum O_i^2}}, \tag{1}$$

where O_i and M_i are the observed and modelled variables. The NRMSE of H_S is equal to 0.137. This value of NRMSE is consistent with the error metrics range reported by recent studies dealing with spectral wave modelling in coastal water [14, 17], thus proving the ability of the adopted approach in modelling nearshore wave dynamics.

4.3.2. Phase-resolving modelling

The spectra obtained as output of the SWAN simulations were used as a boundary conditions for the wave-resolving model XBeach [20] covering the shallow water area. The nonhydrostatic module of XBeach used in this study is based on the nonlinear shallow water equations, including a nonhydrostatic term to account for frequency dispersion in intermediate water. Simulations were setup in 1D cross-shore mode along the two transects T3 and T7, see Figure 8. The numerical domain covered the nearshore area from 14 m of depth up to the toe of the dune system. The seaward boundary with a water depth of 14 m was chosen since it lies in proximity of the outward boundary of surf zone of major storms at Poetto. The choice of the offshore water depth for the 1D XBeach simulations follows from a compromise between two considerations. On one hand it is desirable to have the boundary as close as possible to the shore so that the wave field includes the effects of the refraction processes caught by SWAN. On the other hand, a boundary placed in water too shallow would lead to strong nonlinearities with a large and unrealistic second-order long-wave generation. See also the recent work of Fiedler et al. [21] addressing the role offshore boundary conditions in surf zone modeling.

The mean water level of each XBeach simulation was set according to the level measured by the tidal gauge. To provide a detailed description of swash zone processes, the horizontal spatial grid resolution increased shoreward from 3.5 m in the generation zone up to 0.5 m in the swash zone, see Figure 9. The offshore boundary generated the time series of incoming waves from the SWAN spectrum and absorbed the outgoing waves resulting from beach reflection. The model accounted for friction through the Chezy coefficient setup to 30 $m^{0.5}/s$, which is consistent with previously reported constant friction coefficients of 0.015 [22]. Infiltration/exfiltration processes were simulated by including a constant permeability coefficient of 0.0003 m/s, equal to that measured on the beach berm in presence of reeds. We identify the runup toe as the shoreward point with water depth larger than 0.05 m.

To assess the role played by the reed-reinforced berm in coastal protection, we calculate the storm-induced runup both with an empirical approach and with XBeach modelling. We focus on the aforementioned 12 storms occurred in the period of observation. The total water level TWL is calculated as:

$$TWL = MSL + R_{2\%}, \tag{2}$$

in which MSL is the mean sea level and $R_{2\%}$ is the 2% exceedence level for runup. MSL is obtained from the tide gauge installed inside the Cagliari harbour.

In the empirical approach, the runup contribution to the flooding level is determined from the spectral wave parameters (H_S and T_p) computed by SWAN along the two transects T3 and T7 at a water depth of 14 m. The runup contribution to the flooding elevation is then obtained through:

$$R_{2\%} = 1.1(\langle\eta\rangle + \frac{S}{2}), \tag{3}$$

where $\langle\eta\rangle$ is the wave setup and S is the significant swash. Here, $\langle\eta\rangle$ and S are estimated from H_S, T_p and the foreshore slope β according to Stockdon et al. [23].

$$R_{2\%} = 1.1(0.35\tan\beta(H_0L_0)^{1/2} + \frac{[H_0L_0(0.563\tan\beta^2 + 0.004)]}{2})for\xi_0 \geq 0.3, \tag{4}$$

and

$$R_{2\%} = 0.043(H_0L_0)^{1/2}for\xi_0 < 0.3, \tag{5}$$

where H_0 and L_0 are the deep-water significant wave height and wavelength. ξ_0 is the Iribarren number or surf similarity parameter, computed as:

$$\xi_0 = \frac{\tan\beta}{(H_0L_0)^{1/2}}. \tag{6}$$

In the numerical approach based on XBeach, $R_{2\%}$ is obtained directly from the computed runup time series.

5. Results

The TWL values from the empirical and numerical approaches are compared in Figure 10. TWL calculated with the empirical method and TWL from XBeach are in good agreement. Since both approaches include the same MSL (from the tidal gauge), they can only differ as a result of the runup parameter $R_{2\%}$. This agreement highlights the general reliability of these different methods for runup and flooding calculations. Considering the XBeach output as reference value, the NRMSE of the TWL is equal to 0.235 and 0.179 for transects T3 and T7, respectively. Moreover, Figure 10 is in good

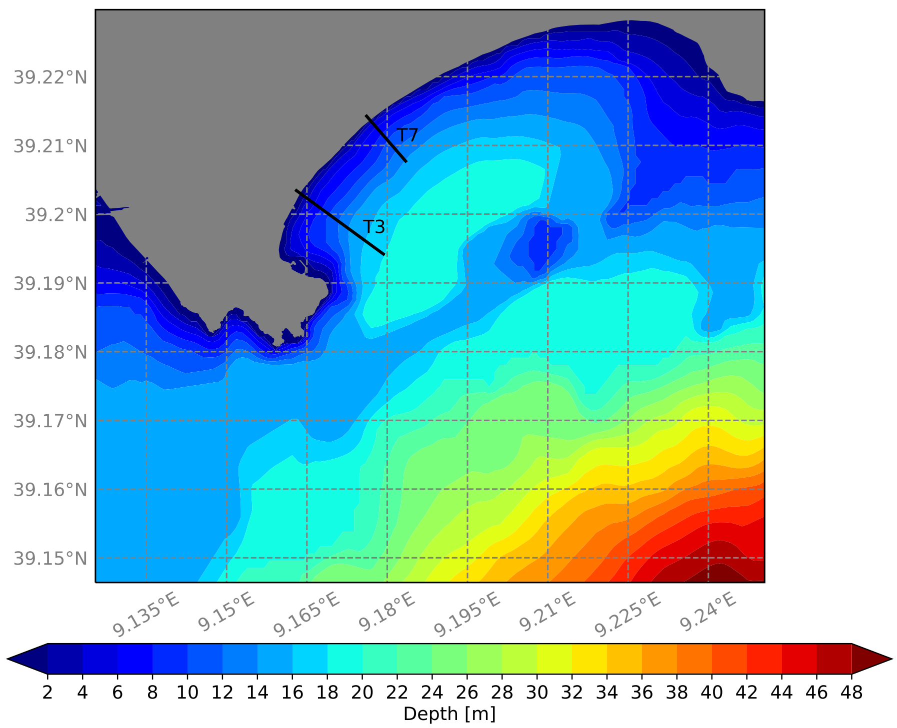

Figure 8: Detail of the bathymetry in the Gulf of Cagliari with the transects T3 and T7.

agreement with visual observations obtained from the video camera system. In fact, the images captured from the video camera revealed significant berm overwash during the S1 and S4; whereas storms S10 and S12 led to isolated overwash events. These four storms are identified as those driving the highest TWL values at the two transects at Poetto beach.

Figure 11 shows the horizontal total water distance TWD from XBeach simulations. Both the TWL and the TWD include the $R_{2\%}$ parameter computed as the 2% exceedence level from the XBeach runup time series. TWL takes into account the vertical runup, whereas the horizontal runup contributes to TWD. The TWD parameter gives an insight of the flooding magnitude that is more difficult to achieve from the vertical TWL. This is mainly due to the fact that large part of the emerged beach lies below the berm elevation. In fact, sea conditions leading to overwash such as S1 and S4 give a TWL only few cm above the berm height, whereas the TWD is few meters beyond the berm crest location, indicated by the dashed line in

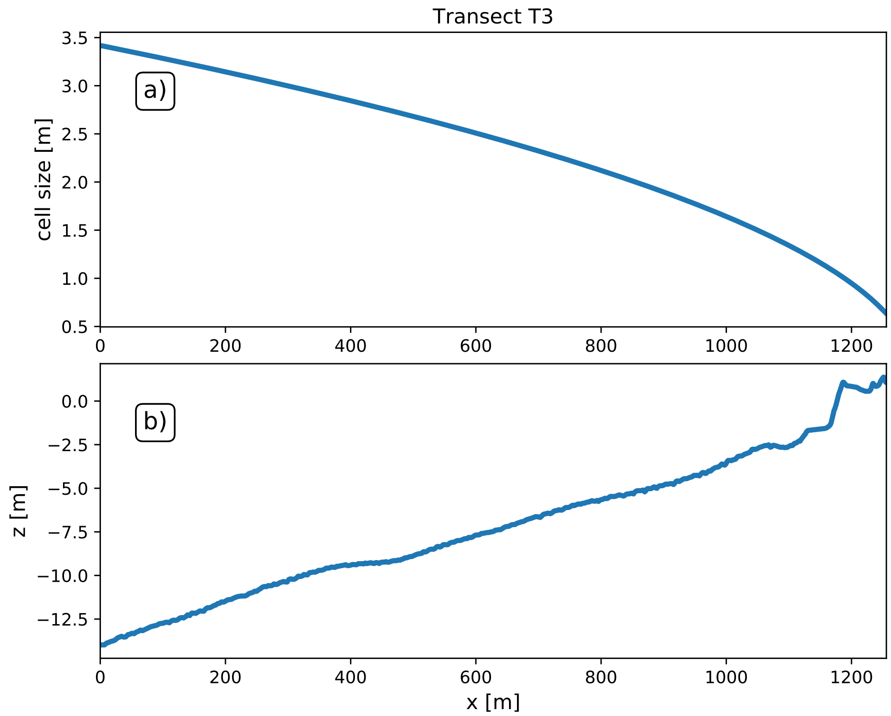

Figure 9: a) Grid size variation across the XBeach computational domain for transect T3. b) Beach profile along T3.

Figure 11. Figure 11 is consistent with Figure 10 allowing the identification of the four storms driving berm overwash. In addition, Figure 11 reveals the difference in flooding magnitude between the most severe storm S4 and the less strong storms S10 and S12.

Figure 12 displays the time series of swash dynamics during storm S1, providing details of overwash dynamics on a low-lying backshore. Panel c) shows that vertical runup does not significantly overcome the berm elevation, although major uprushes are able to drive overwash. Instead, the horizontal runup time series (Figure 12d) allows the identification of uprush events leading to overwash in which the berm crest location is exceeded. The upper panel highlights how effectively the infiltration processes drain the volume of water that overwashes the berm. In the simulation of the storm S1, the water accumulated by an overwash event over the emerged beach is completely drained before the arrival of the next overwash.

To investigate the importance of infiltration processes, we conducted another set of XBeach simulations using the hydraulic conductivity measured on the backshore on the sandy substrate, without the presence of buried reeds. Figure 13 compares the computed flooding induced by the identified storms on the profile with a permeability coefficient of 0.00003 m/s with that computed on the profile with a permeability coefficient of 0.0003 m/s. In other words, the XBeach boundary conditions were the same in the two configurations that differed only in the hydraulic conductivity. To prevent the possible variability linked to wave groupiness [24], not only the spectral shape but also the time series of the boundary conditions were conserved. In general terms, under the same environmental forcing, a lower hydraulic conductivity seems to increase the flooding extension under overwash conditions. The strongest TWD increases are found in run S4 on transect T3 (13 m) and in run S1 on transect T7 (7 m). On the other hand, under moderate wave conditions without overwash, infiltration processes have no significant effect of runup and TWD values.

The assessment of beach flooding through a numerical approach shows that four storms (S1, S4, S10 and S12) drove berm overwash during the observation period. Storms S1 and S4 led to significant overwash and flooding, whereas storms S10 and S12 produced only isolated overwash events with limited beach flooding. These results confirm the analysis of the images obtained from the video-monitoring system (the video-monitoring system did not detect overwash under storm S12 probably because this event happened at night and the moderate overwash left no visible marks on the beach). Under energetic conditions, once the berm is overwashed, the relative depression in the beach geometry favours the beach flooding towards the dune system. Numerical simulations conducted with different hydraulic conductivity coefficients allow the assessment of the role played by beach permeability on runup and flooding. According to previous studies [25] suggesting that on sandy beaches weak infiltration processes are not able to modify swash dynamics, no appreciable differences in runup are found for moderate wave conditions in which the swash zone does not exceed the berm crest. Nevertheless, the results suggest that a low permeability coefficient tends to increase flooding under severe forcing leading to overwash. This process can be observed in Figure 14 showing the comparison of two snapshots taken at the same moment in which a wave is overwashing the berm from the XBeach simulations of storm S1. The difference in permeability does not yield appreciable changes in the runup location (indicated by the red dot) in proximity of the

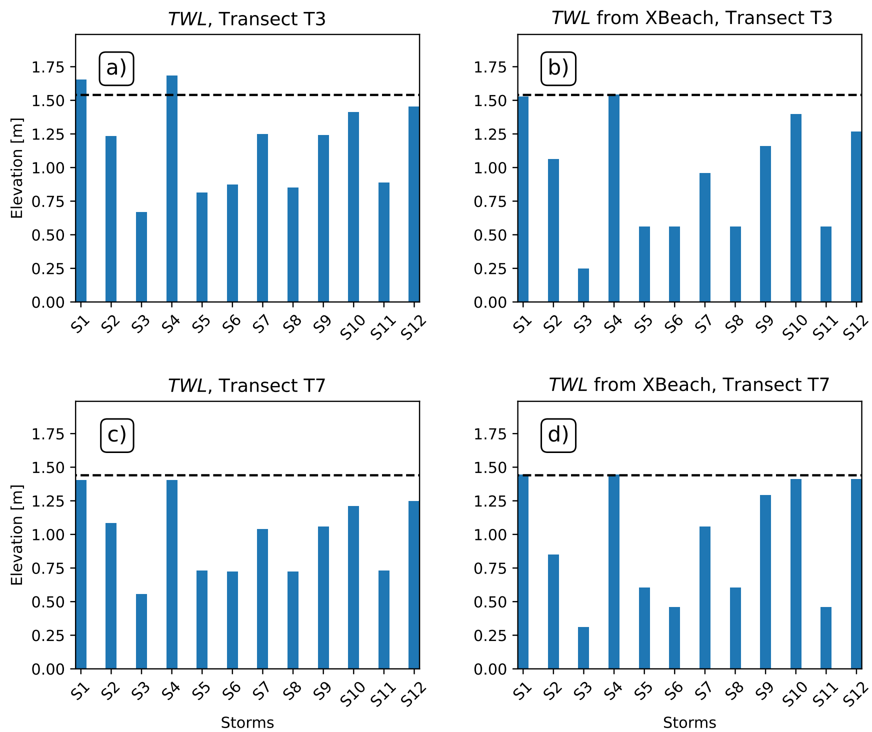

Figure 10: Total water level TWL using parametric formulas for runup (a and c) and from XBeach simulations (b and d). The dashed line is the beach berm height above mean sea level.

berm. At the same time, the panel c) of the figure highlights how the low permeability precludes a complete evacuation of the water from the emerged beach. The water that overwashes the berm tends to accumulate on the emerged beach, eventually increasing the flooding area.

The simulations carried out so far have considered a homogeneous friction factor (Chezy equal to 30 $m^{0.5}/s$) over the entire beach profile. However, it is plausible that seagrass and reed deposits can enhance friction dissipation by increasing roughness at the bed. To quantify possible implications for coastal flooding, we have run a new set of simulations in which the friction was increased in the region of the profile covered with wracks over the T3 profile (we did not consider T7 since it is not in the area monitored from the video camera system). On the day in which the topographic survey was conducted, the videocamera system showed seagrass and reed wracks deposits

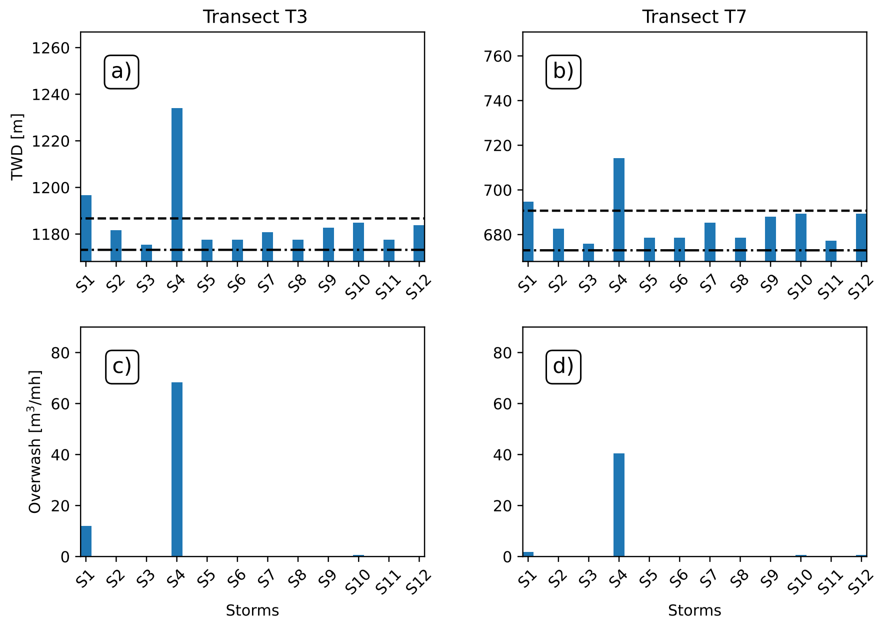

Figure 11: a) and b) Horizontal total water distance from XBeach simulations. The dashed line and the dot-dashed line are the cross-shore location of the beach berm crest and the mean water level, respectively. c) and d) Overwash rate

that extended over 5 m landward from the berm of the profile of transect T3. The Chezy friction coefficient was set to 10 $m^{0.5}/s$ over this area, a value chosen according to Chow [26] (vegetal lining). The permeability and other parameters were kept constant as in the previous simulations. Whereas the TWD induced by the most energetic storm S4 is not affected by the change in friction, a slightly reduction of 1 m is observed only for run S1 (not shown). This may be related to the flooding extension whose landward limit falls in proximity of the wracks in run S1. As expected, the locally-increased friction does not yield any TWD change under moderate storm conditions in which no overwash occurs.

6. Discussion

The approach followed in this work allows the assessment of runup and flooding on a low-lying backshore following an exceptional event of reed (*Arundo donax*) deposition. Particular attention is devoted to the overwash

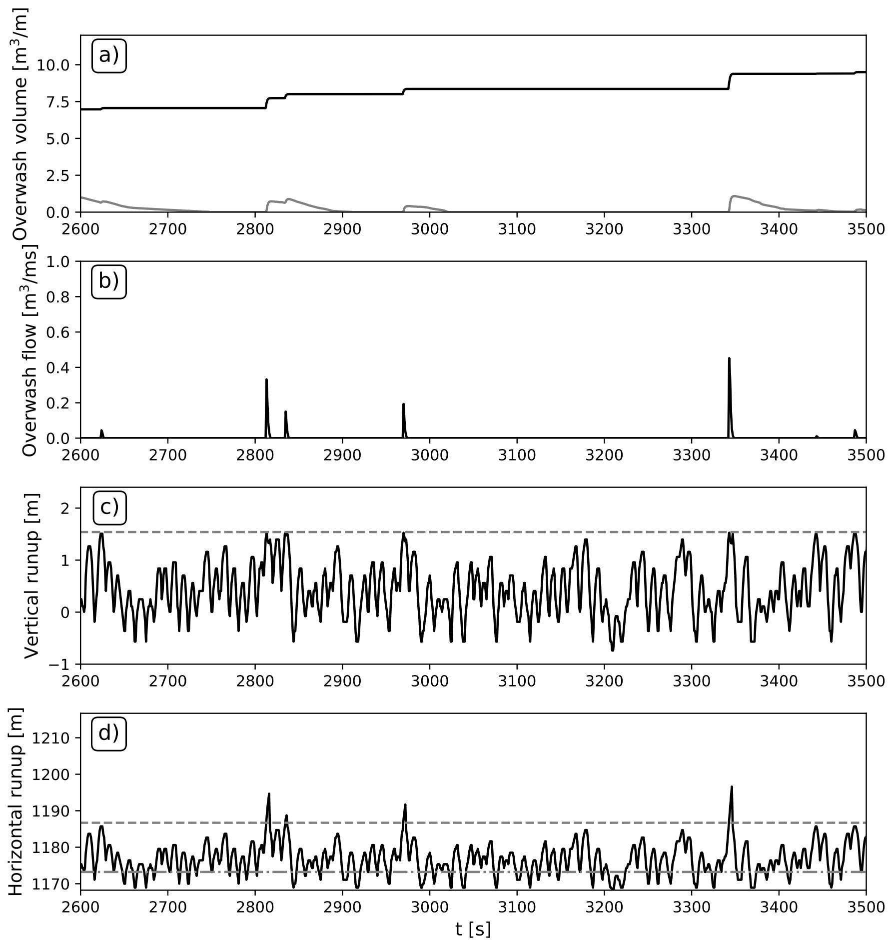

Figure 12: Time series of swash dynamics. a) The black line is the cumulative overwash volume; the gray line is the water volume accumulated over the emerged beach. b) Instantaneous overwash flow. c) Vertical runup. The dashed line is the berm crest elevation. d) Horizontal runup. The dashed line is the berm crest location, whereas the dot-dashed line is the intersection between the mean water level and the beach profile.

dynamics over the berm and to the infiltration processes occurring on the emerged beach. This section discusses the implications of the results together with the limitations and assumptions related to the adopted methodology.

We estimate the runup and flooding at Poetto beach through a model chain with increasing spatial resolution. The model chain, with the nesting of a phase-resolving model into a phase-averaged model, provides an

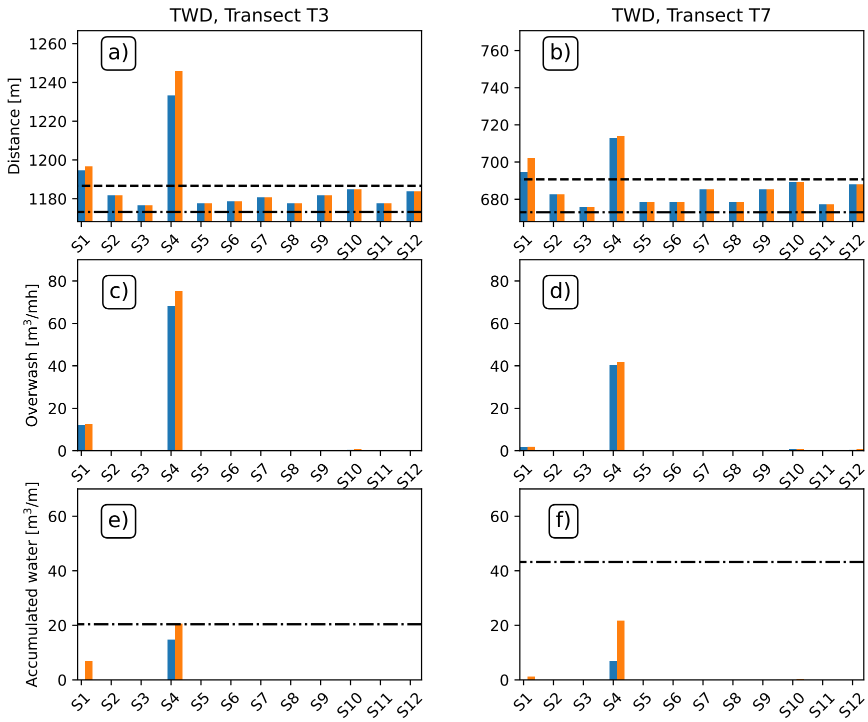

Figure 13: Comparison of the results from XBeach simulations using the permeability coefficient of 0.0003 m/s (blue) and using the permeability coefficient of 0.00003 m/s (orange). a) and b) Horizontal total water distance TWD. The dashed line is the berm crest location, whereas the dot-dashed line is the intersection between the mean water level and the beach profile. c) and d) Cumulative overwash volume. e) and f) Accumulated water volume over the emerged beach at the end of the simulation. The dot-dashed line is the maximum water volume that can be stored between the berm and the dune system.

accurate characterization of the main nearshore and shallow water processes driving wave runup dynamics, limiting the number of assumptions involved. However, few assumptions are still present in the XBeach simulation setup. For instance, the cross-shore configuration precludes the characterization of longshore dynamics. The validity of the cross-shore approach in surf zone modelling has been extensively addressed by Fiedler et al. [27, 21]. In particular Fiedler et al. [27] tested the 1D assumption and concluded that it is a reasonable assumption for the prediction the bulk properties of runup observed on natural beaches for a wide range of incident wave conditions. In fact, as long as the offshore boundary of the 1D model lies outside the

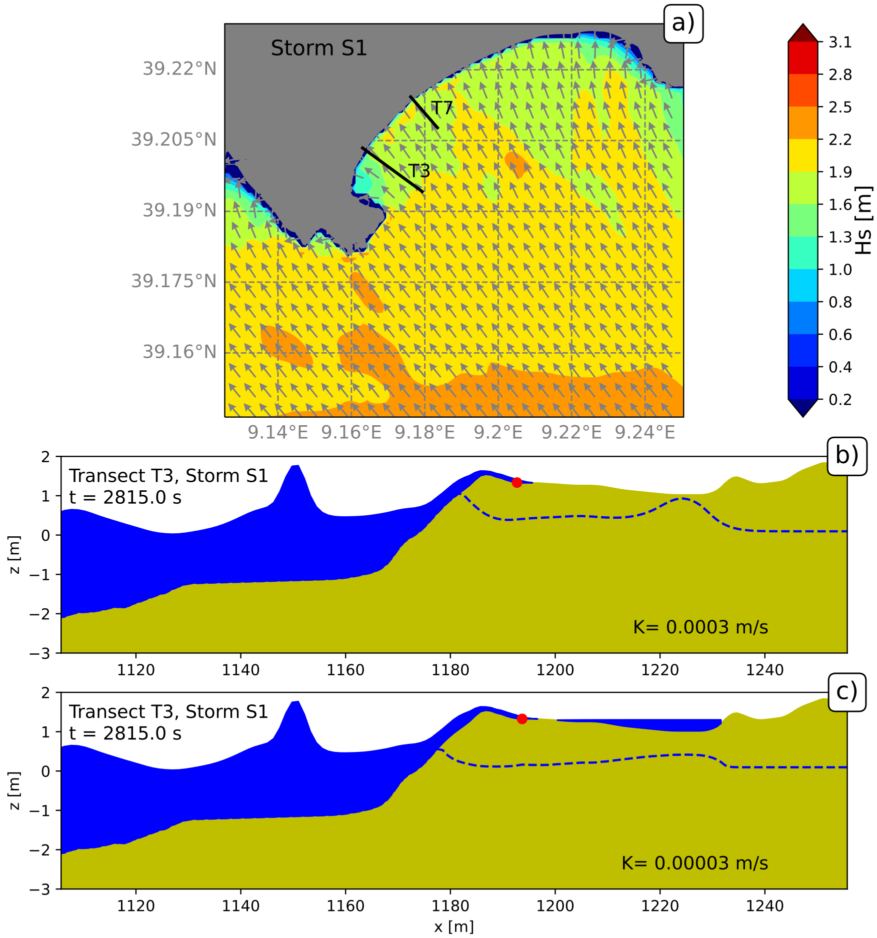

Figure 14: a) Significant wave height field computed by SWAN for storm S1. b) and c) Snapshot of the XBeach simulations for Storm S1 along the transect T3 with a permeability coefficient (K) equal to 0.0003 m/s and 0.00003 m/s, respectively. The red dot shows the moving shoreline (runup) location. The blue dashed line indicates the groundwater table elevation.

surf zone but sufficiently close to the shoreline (in this study it lies at a point with 14 m depth), refraction processes of shoaling waves lead to a near normal wave incidence at this boundary.

A good agreement is found between the vertical runup values calculated with the empirical formulation by Stockdon et al. [23] and those computed with XBeach, see Figure 10. Among different runup formulations that have been proposed during the last decades [28, 29], we have chosen to apply the Stockdon et al. [23] formulation due to its wide diffusion within the coastal engineering community [30, 31]. Although empirical formulations still lack to address the effects induced by complex nearshore morphology [32, 33] and by incoming wave features [34, 35], they have proven to provide a first order assessment of wave runup under a wide range of wave and environmental conditions [36]. This justifies their use for a first order assessment of runup in those situations in which the use a phase-resolving model is not recommended, for instance for operational systems whose routines are run daily and computational efficiency is of paramount importance [18].

Previous studies have reported highly dynamic banquettes that evolve, form and recede according to the wave forcing variability [37, 8, 38, 9]. Although the evolution of beach-cast *Posidonia oceanica* litter has been widely reported, fewer studies have addressed dynamics of small woody debris and reed deposits. Gómez-Pujol et al. [38] and Trogu et al. [9] showed that the permanence of banquettes on wave-exposed beaches is transitory and these features hardly withstand energetic storms. This variability raises doubts about the effective coastal protection offered by seagrass wracks under storm conditions. Nevertheless, observations of the berm dynamics during the winter and spring 2019-2020 at Poetto suggest that major storms are able to shift shoreward the organic berm location but not to dismantle it (see Figure 15 showing the presence of reed wracks both before and at the end of storm S4). In other words, the presence of intertwined reeds and seagrasses within the beach berm seems to increase its flexibility and preserve it against destructive wave action. More detailed analyses on the variability of the extension of reed and seagrass wracks according to wave and environmental forcing will be presented in a future paper.

Since the larger permeability coefficients have been found in areas with sand mixed with buried reeds, this result suggests that intertwined reed and seagrass wracks can mitigate the effects of overwash and flooding by increasing the beach permeability, promoting infiltration and thus water evacuation from the emerged beach. In this study, the effects of a locally-increased bottom friction by reed ad seagrass deposits seems to have a limited and secondary impact on coastal flooding. The discussed assumptions involved in this study, such as the use of a single permeability coefficient over the entire beach profile, suggest that these findings should be confirmed by more refined and more exhaustive swash modelling in future works.

In terms of coastal protection from flooding, these results suggest that

Figure 15: View of the Poetto beach from the video camera system. a) picture taken before S4 storm (19/01/2020); b) picture taken at the tail of S4 storm (24/01/2020).

keeping the reed deposits in place appears as a sound solution. The reed deposits can be regarded as an ecosystem-based solution and their services be should be taken into account in a sustainable coastal planning strategy. At the same time, it is evident that these barriers of dead plants on Mediterranean beaches considerably limit the suitability for bathing. Therefore, in these cases, their removal must be considered, creating the problem of reconciling environmental protection and tourist use. In this context, making available to local authorities an assessment of how the reed and seagrass deposition affects coastal processes can be beneficial towards a sustainable coastal management. In principle, the the same approach adopted by the legislation for the *Posidonia oceanica* management can be extended to reed wracks: keeping the biomass in place, compatibly with the touristic vocation of a specified beach. In fact, the intertwined reed and seagrass wracks have the effect of increasing the permeability of the beach, thus favouring the drainage of water from the emerged beach, eventually reducing flooding. Nevertheless, in this particular case, the touristic vocation of Poetto beach precluded the possibility of keeping the huge amount of reed deposits in place, as they constituted a significant obstacle in terms of beach fruition and shoreline accessibility.

7. Conclusions

This work devotes a special attention to runup processes induced by storms at a low-lying backbeach in the presence of reed and seagrass deposits. The methodology included a model chain with increasing spatial resolution and details. Data showed that, due to the beach profile with the berm higher than the emerged beach, the horizontal runup provided a quantification of the flooding extension that is more difficult to achieve from the vertical runup. Using the hydraulic conductivity parameter measured in a beach area with sand and buried reeds, infiltration processes allowed the beach to drain the overwashed water and its return to the sea. The role of beach permeability on runup was assessed by running a new set of wave simulations using a low hydraulic conductivity parameter, equal to that measured in a beach area with sand only. Under overwash conditions, runup and flooding extensions were increased by a low permeability coefficient. These results highlight the role of the ecosystem services provided by intertwined reed and seagrass wracks on beaches, suggesting that they must be taken into account in a sustainable coastal planning strategy.

Acknowledgement

This work was supported by Regione Autonoma Sardegna under L.R. 7/2007, "Promozione della ricerca scientifica e dell'innovazione tecnologica in Sardegna" for BEACH, TENDER NEPTUNE and NEPTUNE 2 projects directed by Sandro De Muro. Daniele Trogu acknowledges the support by the University of Cagliari ("Borse di studio di Ateneo"-Dottorati di Ricerca XXXIV ciclo, voce CO.AN.A.06.01.01.01.01.02).

The authors warmly thank Battellieri Cagliari and Sardegna Progetta for their assistance during the field work. The authors would like to thank the Sardinia Sea Port Authority, the "Deposito PolNato Marina Militare (Navy PolNato Depot Marina Militare)" of Cape S. Elia–Cagliari and Comando supporto logistico di Cagliari (MARICAGLIARI). Sincere thanks go to the Comune di Cagliari (Alessandro Guarracino) for having allowed the seasonal monitoring survey during the pandemic lockdown.

This study has been conducted using E.U. Copernicus Marine Service Information.

References

[1] Y. Pan, M. Flindt, P. Schneider-Kamp, M. Holmer, Beach wrack mapping using unmanned aerial vehicles for coastal environmental management, Ocean and Coastal Management 213 (2021) 105843. URL: `https://www.sciencedirect.com/science/article/pii/S0964569121003264`. doi:https://doi.org/10.1016/j.ocecoaman.2021.105843.

[2] J. B. Eamer, I. J. Walker, Quantifying sand storage capacity of large woody debris on beaches using lidar, Geomorphology 118 (2010) 33–47. URL: `https://www.sciencedirect.com/science/article/pii/S0169555X09005224`. doi:https://doi.org/10.1016/j.geomorph.2009.12.006.

[3] M. J. Grilliot, I. J. Walker, B. O. Bauer, The role of large woody debris in beach-dune interaction, Journal of Geophysical Research: Earth Surface 124 (2019) 2854–2876. doi:https://doi.org/10.1029/2019JF005120.

[4] D. M. Kennedy, J. L. Woods, The influence of coarse woody debris on gravel beach geomorphology, Geomorphology 159-160 (2012) 106–115. URL: `https://www.sciencedirect.com/science/article/pii/S0169555X12001274`. doi:https://doi.org/10.1016/j.geomorph.2012.03.009.

[5] S. Tecchiato, C. Buosi, A. Ibba, D. A. Ryan, S. D. Muro, A Comparison of Geomorphic Settings, Sediment Facies and Benthic

Habitats of Two Carbonate Systems of Western Mediterranean Sea and South Western Australia: Implications for Coastal Management, Journal of Coastal Research 75 (2016) 562 – 566. URL: https://doi.org/10.2112/SI75-113.1. doi:10.2112/SI75-113.1.

[6] S. De Muro, S. Tecchiato, C. Buosi, M. Porta, M. Bachis, A. Ibba, Geomorphology, Sedimentology, Benthic Habitat as Tools For Supporting Coastal Management: Comparison Between Australian And Mediterranean Beach Systems, Journal of Coastal Research 85 (2018) 1526 – 1530. URL: https://doi.org/10.2112/SI85-306.1. doi:10.2112/SI85-306.1.

[7] M. Vacchi, G. De Falco, S. Simeone, M. Montefalcone, C. Morri, M. Ferrari, C. N. Bianchi, Biogeomorphology of the mediterranean posidonia oceanica seagrass meadows, Earth Surface Processes and Landforms 42 (2017) 42–54. doi:https://doi.org/10.1002/esp.3932.

[8] S. Simeone, S. De Muro, G. De Falco, Seagrass berm deposition on a mediterranean embayed beach, Estuarine, Coastal and Shelf Science 135 (2013) 171–181. URL: https://www.sciencedirect.com/science/article/pii/S0272771413004460. doi:https://doi.org/10.1016/j.ecss.2013.10.007.

[9] D. Trogu, C. Buosi, A. Ruju, M. Porta, A. Ibba, S. De Muro, What Happens to a Mediterranean Microtidal Wave-dominated Beach During Significant Storm Events? The Morphological Response of a Natural Sardinian Beach (Western Mediterranean), Journal of Coastal Research 95 (2020) 695 – 700. URL: https://doi.org/10.2112/SI95-135.1. doi:10.2112/SI95-135.1.

[10] A. McLachlan, O. Defeo, E. Jaramillo, A. D. Short, Sandy beach conservation and recreation: Guidelines for optimising management strategies for multi-purpose use, Ocean and Coastal Management 71 (2013) 256–268. URL: https://www.sciencedirect.com/science/article/pii/S0964569112002761. doi:https://doi.org/10.1016/j.ocecoaman.2012.10.005.

[11] C. Battisti, G. Fanelli, A. Filpa, F. Cerfolli, Giant reed (arundo donax) wrack as sink for plastic beach litter: First evidence and implication, Marine Pollution Bulletin 155 (2020) 111179. URL:

https://www.sciencedirect.com/science/article/pii/S0025326X20302976. doi:https://doi.org/10.1016/j.marpolbul.2020.111179.

[12] S. De Muro, A. Ibba, S. Simeone, C. Buosi, W. Brambilla, An integrated sea-land approach for mapping geomorphological and sedimentological features in an urban microtidal wave-dominated beach: a case study from s sardinia, western mediterranean, Journal of Maps 13 (2017) 822–835. doi:10.1080/17445647.2017.1389309.

[13] M. Biondo, C. Buosi, D. Trogu, H. Mansfield, M. Vacchi, A. Ibba, M. Porta, A. Ruju, S. De Muro, Natural vs. anthropic influence on the multidecadal shoreline changes of mediterranean urban beaches: Lessons from the gulf of cagliari (sardinia), Water 12 (2020). URL: https://www.mdpi.com/2073-4441/12/12/3578.

[14] M. Ravdas, A. Zacharioudaki, G. Korres, Implementation and validation of a new operational wave forecasting system of the mediterranean monitoring and forecasting centre in the framework of the copernicus marine environment monitoring service, Natural Hazards and Earth System Sciences 18 (2018) 2675–2695. URL: https://nhess.copernicus.org/articles/18/2675/2018/. doi:10.5194/nhess-18-2675-2018.

[15] M. Mathiesen, Y. Goda, P. J. Hawkes, E. Mansard, M. J. Martin, E. Peltier, E. F. Thompson, G. V. Vledder, Recommended practice for extreme wave analysis, Journal of Hydraulic Research 32 (1994) 803–814. doi:10.1080/00221689409498691.

[16] M. Zijlema, A. J. van der Westhuysen, On convergence behaviour and numerical accuracy in stationary swan simulations of nearshore wind wave spectra, Coastal Engineering 52 (2005) 237–256. URL: https://www.sciencedirect.com/science/article/pii/S0378383904001681. doi:https://doi.org/10.1016/j.coastaleng.2004.12.006.

[17] G. Bellotti, L. Franco, C. Cecioni, Regional downscaling of copernicus era5 wave data for coastal engineering activities and operational coastal services, Water 13 (2021). URL: https://www.mdpi.com/2073-4441/13/6/859. doi:10.3390/w13060859.

[18] K. Stokes, T. Poate, G. Masselink, E. King, A. Saulter, N. Ely, Forecasting coastal overtopping at engineered and naturally defended coastlines, Coastal Engineering 164 (2021) 103827. URL: https://www.sciencedirect.com/science/article/pii/S0378383920305135. doi:https://doi.org/10.1016/j.coastaleng.2020.103827.

[19] A. Ruju, M. Passarella, D. Trogu, C. Buosi, A. Ibba, S. De Muro, An operational wave system within the monitoring program of a mediterranean beach, Journal of Marine Science and Engineering 7 (2019). URL: https://www.mdpi.com/2077-1312/7/2/32. doi:10.3390/jmse7020032.

[20] D. Roelvink, R. McCall, S. Mehvar, K. Nederhoff, A. Dastgheib, Improving predictions of swash dynamics in xbeach: The role of groupiness and incident-band runup, Coastal Engineering 134 (2018) 103–123. URL: https://www.sciencedirect.com/science/article/pii/S0378383917301321. doi:https://doi.org/10.1016/j.coastaleng.2017.07.004, rISC-KIT: Resilience-increasing Strategies for Coasts – Toolkit.

[21] J. W. Fiedler, P. B. Smit, K. L. Brodie, J. McNinch, R. Guza, The offshore boundary condition in surf zone modeling, Coastal Engineering 143 (2019) 12–20. URL: https://www.sciencedirect.com/science/article/pii/S0378383918301984. doi:https://doi.org/10.1016/j.coastaleng.2018.10.014.

[22] B. Raubenheimer, R. T. Guza, S. Elgar, N. Kobayashi, Swash on a gently sloping beach, Journal of Geophysical Research: Oceans 100 (1995) 8751–8760. doi:https://doi.org/10.1029/95JC00232.

[23] H. F. Stockdon, R. A. Holman, P. A. Howd, A. H. Sallenger, Empirical parameterization of setup, swash, and runup, Coastal Engineering 53 (2006) 573 – 588. doi:https://doi.org/10.1016/j.coastaleng.2005.12.005.

[24] J. Rutten, A. Torres-Freyermuth, J. Puleo, Uncertainty in runup predictions on natural beaches using xbeach nonhydrostatic, Coastal Engineering 166 (2021) 103869. URL: https://www.sciencedirect.com/science/article/pii/S0378383921000296. doi:https://doi.org/10.1016/j.coastaleng.2021.103869.

[25] G. Masselink, L. Li, The role of swash infiltration in determining the beachface gradient: a numerical study, Marine Geology 176 (2001) 139–156. URL:

https://www.sciencedirect.com/science/article/pii/S002532270100161X. doi:https://doi.org/10.1016/S0025-3227(01)00161-X.

[26] V. Chow, Open-Channel Hydraulics, McGraw-Hil, 1959.

[27] J. W. Fiedler, P. B. Smit, K. L. Brodie, J. McNinch, R. Guza, Numerical modeling of wave runup on steep and mildly sloping natural beaches, Coastal Engineering 131 (2018) 106–113. URL: https://www.sciencedirect.com/science/article/pii/S037838391730193X. doi:https://doi.org/10.1016/j.coastaleng.2017.09.004.

[28] A. L. Atkinson, H. E. Power, T. Moura, T. Hammond, D. P. Callaghan, T. E. Baldock, Assessment of runup predictions by empirical models on non-truncated beaches on the south-east australian coast, Coastal Engineering 119 (2017) 15 – 31. URL: http://www.sciencedirect.com/science/article/pii/S037838391630285X. doi:https://doi.org/10.1016/j.coastaleng.2016.10.001.

[29] M. Passarella, E. B. Goldstein, S. De Muro, G. Coco, The use of genetic programming to develop a predictor of swash excursion on sandy beaches, Natural Hazards and Earth System Sciences 18 (2018) 599–611. URL: https://www.nat-hazards-earth-syst-sci.net/18/599/2018/. doi:10.5194/nhess-18-599-2018.

[30] A. Tomas, F. Mendez, R. Medina, F. Jaime, P. Higuera, J. Lara, M. Ortiz, M. Alvarez de Eulate, A methodology to estimate wave-induced coastal flooding hazard maps in spain, Journal of Flood Risk Management 9 (2016) 289–305. doi:10.1111/jfr3.12198.

[31] N. Cohn, P. Ruggiero, The influence of seasonal to interannual nearshore profile variability on extreme water levels: Modeling wave runup on dissipative beaches, Coastal Engineering 115 (2016) 79 – 92. URL: http://www.sciencedirect.com/science/article/pii/S0378383916000168. doi:https://doi.org/10.1016/j.coastaleng.2016.01.006, swash-zone Processes.

[32] N. Cox, L. M. Dunkin, J. L. Irish, An empirical model for infragravity swash on barred beaches, Coastal Engineering 81 (2013) 44–50. URL:

https://www.sciencedirect.com/science/article/pii/S0378383913001178. doi:https://doi.org/10.1016/j.coastaleng.2013.06.008.

[33] R. M. Guedes, K. R. Bryan, G. Coco, Observations of alongshore variability of swash motions on an intermediate beach, Continental Shelf Research 48 (2012) 61–74. URL: https://www.sciencedirect.com/science/article/pii/S027843431200249X. doi:https://doi.org/10.1016/j.csr.2012.08.022.

[34] R. T. Guza, F. Feddersen, Effect of wave frequency and directional spread on shoreline runup, Geophysical Research Letters 39 (2012). doi:10.1029/2012GL051959.

[35] A. Ruju, J. L. Lara, I. J. Losada, Numerical assessment of infragravity swash response to offshore wave frequency spread variability, Journal of Geophysical Research: Oceans 124 (2019) 6643–6657. doi:https://doi.org/10.1029/2019JC015063.

[36] M. Passarella, S. De Muro, A. Ruju, G. Coco, An Assessment of Swash Excursion Predictors using Field Observations, Journal of Coastal Research 85 (2018) 1036 – 1040. URL: https://doi.org/10.2112/SI85-208.1. doi:10.2112/SI85-208.1.

[37] S. Simeone, G. De Falco, Morphology and composition of beach-cast posidonia oceanica litter on beaches with different exposures, Geomorphology 151-152 (2012) 224–233. URL: https://www.sciencedirect.com/science/article/pii/S0169555X12000700. doi:https://doi.org/10.1016/j.geomorph.2012.02.005.

[38] L. Gómez-Pujol, A. Orfila, A. Álvarez Ellacuría, J. Terrados, J. Tintoré, Posidonia oceanica beach-cast litter in Mediterranean beaches: a coastal videomonitoring study, Journal of Coastal Research 65 (2013) 1768 – 1773. URL: https://doi.org/10.2112/SI65-299.1. doi:10.2112/SI65-299.1.